Defence Science Journal, Vol. 75, No. 5, September 2025, pp. 629-636, DOI: 10.14429/dsj.20343


# Influence of Raster Angle and Infill Pattern on the Mechanical Performance of Additively Manufactured Carbon Fiber Composite

Ashok Kumar[#,*] and Ashwin Kumar[$]

[#]*Cyprus Marine and Maritime Institute, Larnaca – 6023, Republic of Cyprus*
[$]*Department of Mechanical Engineering, SRM Easwari Engineering College, Chennai - 600 089, India*
[*]*E-mail: s.ashokji@gmail.com*

**ABSTRACT**

The growing demand for high-specific strength, lightweight materials drives research and innovation in manufacturing industries. Composite materials are emerging as viable alternatives to traditional metals and alloys as they address these critical industry requirements effectively. Advancements in additive manufacturing technology have transformed the fabrication of composite materials with tailored mechanical properties. However, there is a limited understanding of the material properties of composites manufactured through three-dimensional (3D) printing technology. This work aims to provide a better understanding of the relationship between the 3D printing process parameters and mechanical properties of the carbon fibre materials. Specifically, the study reports the effect of raster angle and infill pattern on the flexural and impact properties of onyx-reinforced carbon fibre composites. Major findings from this study reveal that there is a significant decrease in flexural strength with an increase in raster angle due to parallel deposition of fibres. In addition, the triangular infill pattern had the highest energy absorption when compared to all other equivalents. The 0° raster angles with solid or rectangular infill patterns and 45º raster angles with triangular or solid patterns are ideal for applications with high flexural strength and impact resistance, respectively.

**Keywords:** Fibre reinforced polymer; 3D printing, Flexural strength; Raster angle; Infill pattern; Impact analysis

## 1. INTRODUCTION

The relentless pursuit of lightweight, high-performance materials remains crucial for innovation and advancement in aerospace, maritime and automotive industries, where the weight of the component plays a crucial role in the operation of the system. Composite materials play an important role in this endeavour, which allows the combining properties of multiple materials. However, traditional composite manufacturing methods offer less design flexibility and intricacy, the need for skilled personnel and high capital investments

Additive Manufacturing (AM) of reinforced thermoplastics has revolutionised the manufacturing industry. In the American Standard of Testing Materials (ASTM) Society, AM is defined as the process of joining materials layer by layer to create physical objects from 3D Computer-Aided Design (CAD) model data[1]. The advantages of composites are further enhanced by AM, which makes it feasible to create complex geometries and optimise material distribution to achieve desired structural properties. This technology allows for precise control over the orientation and alignment of continuous fibres paving the way for the fabrication of architected composites. Integrating 3D printing with composite materials can produce lightweight, strong, improved noise and vibration properties and highly tailored components for various applications ranging from fighter aircraft to prosthetics. Carbon fibre-reinforced polymer (CFRP) composites are prevalent in aircraft control surfaces, fuselages and brake systems. For example, the brake systems of commercial aircraft like Boeing 737 NG[2] and fuselage and stabilizers of Lockheed Martin F-35 are made of CFRPs for superior performance and handling advantages[3]. Similarly, in the automotive industry, composites contribute to improved crashworthiness and fuel efficiency[4].

Composite materials are gaining extensive demand in maritime applications such as propellers, hatch covers, hulls, masts, and bulkheads. Composite propellers have proved efficient than their metallic counterpart in both hydrodynamic and structural aspects. The deflection created due to the hydrodynamic loads during operation has modified the blade profile, thereby improving the propulsive efficiency[5].

The mechanical properties of the 3D-printed thermoplastics depend heavily on certain process parameters. This includes build orientation[6], number of fibre layers[7], fibre volume percentage[8], infill pattern[9], layer thickness[10], raster angle[11], and extrusion temperature[12]. An infill pattern is defined as the geometric shape or pattern in which the materials are deposited inside the printed object. Common infill patterns include grid, triangular, honeycomb, rectilinear, circular, and Gilbert curves. In addition, raster angle is defined as the direction in which fibre reinforcement is deposited within each layer.

Pyl[11], *et. al.* investigated the effect of various raster angles ([0°], [0°/90°], [0°/90°/±45°], [±45°]) of carbon fibre-

Received : 01 July 2024, Revised : 10 April 2025
Accepted : 26 May 2025, Online published : 01 September 2025

reinforced nylon composite, comparing it with traditionally manufactured composite. Martin[13], *et al*. explored the effect of fibre orientation lines on the tensile properties of both Glass fibre and carbon fibre-reinforced nylon composites. He studied 45°-45,0°-0°, 45°-90° and 90°-0°. He identified that fibre orientation significantly impacted the composites' tensile strength.

Srinivasan[14], *et. al.* compared the effect of different infill patterns on the tensile properties of composites, finding that the grid pattern exhibited superior tensile strength compared to triangular, honeycomb, and rectilinear patterns. Ning[15], *et al*. investigated the effect of carbon fibre content and length on tensile strength, finding a significant increase in tensile strength and Young's modulus with higher carbon fibre content and length.

Previous studies have mainly examined the influence of process parameters on tensile properties, while only limited literature is available on flexural and impact properties. Ghebretinsae et al. fabricated onyx carbon fibre composite samples with solid infill (100 % infill density) to examine their flexural properties alongside tensile properties[16]. Hu[17], *et al*. aimed to better understand the flexural behaviour of PLA-reinforced carbon fibre composites by analysing the influence of print temperature, print speed, and layer thickness. According to their findings, layer thickness significantly impacts flexural properties, with thin layers producing superior results. Print speed and temperature had a minimal influence compared to layer thickness.

Impact property literature on fibre-reinforced thermoplastics was even less than the limited flexural property literature. Prajapati[18], *et al.* focused on the influence of fibre layers on the impact strength of onyx glass fibre composite, and they identified that with an increase in the number of layers, there was a significant increase in impact strength. Hetrick[19] conducted a charpy impact test on onyx-reinforced Kevlar fibre to determine the optimal fibre stacking sequence and analyzed their failure modes. It was found from the above literature data that the impact resistance of the 3D printed structure is highly dependent on the mesostructure geometry. The mesostructure is a function of the infill density and the infill pattern.

The mechanical characteristics of 3D printed items made by material extrusion of polyamide-based filament reinforced with 15 % chopped carbon fibres and three different infill patterns-grid, triangle, and lines-with a 50 % infill density are examined[20]. Following specimen testing, the grid infill pattern had the lowest average value across the two mechanical test types; however, the values are larger than in the literature. Tarfaoui[21], *et al.* studied investigated the tensile properties of 3D-printed polyethene terephthalate specimens reinforced with carbon fibre for two infill patterns and four densities. Three infill densities-20 %, 50 %, and 75 %-were used to compare rectilinear and honeycomb infill designs at 100 %.

As expected, the results showed that the tensile strengths and Young's moduli of all examined infill patterns rose in tandem with the infill densities. The design with the maximum tensile strength and Young's modulus has a 75 % honeycomb and 100 % infill density. The honeycomb was the perfect infill pattern with 75 % and 100 % densities, offering great strength and stiffness.

Investigating the mechanical and dynamic behaviours of 3D-printed composite structures under tensile and impact testing was conducted[22]. Onyx layers, triangle infill patterns (30 % and 40 % infill density), and continuous carbon fibre layers (two, four, six, and eight layers) are among the designed sample kinds. Scanning electron microscopy (SEM) and X-ray micro-computed tomography (μCT) investigations visualised the morphological characterisation and the delamination and damage of the composite structures. The study's findings showed that adding layers of carbon fibre reinforcement improves the composite constructions' tensile strength and stiffness.

From the aforementioned literature, it is evident that a crucial gap remains in understanding how infill patterns and raster angles affect the flexural and impact behaviour of onyx-reinforced carbon fibre composites. Limited research has specifically addressed these properties in this particular material combination. There is a necessity to understand the effects of these two critical properties due to its practical application in aerospace maritime and automotive industries.

Hence the present work aims to bridge this knowledge gap by systematically investigating the effects of four distinct infill patterns (grid, triangular, honeycomb, and rectilinear) and three different raster angles (0°, 45°, and 90°) on the flexural and impact properties of onyx-reinforced carbon fibre composites using experimental methods.

## 2. METHODOLOY

The testing specimens were fabricated using a Mark forged Mark-II industrial-grade carbon fibre 3D printer. It uses continuous filament fabrication technology similar to that of FDM but has the additional capability to add reinforcement material into the polymer matrix. This printer has two nozzles, each with its own extrusion head and filament spool. One lays down the matrix filament (Onyx), while the other deposits a continuous composite material (Carbon fibre) strand. A continuous set of carbon fibres was reinforced within onyx, a nylon polymer embedded with micro-chopped carbon fibres for sample preparation. Figure 1 depicts the image of the actual machine used for the fabrication process.

**Figure 1. Image of the 3D printer machine used for the coupon fabrication.**

For the current study, the temperature of the printing heads for Onyx and carbon fibre were set to 275 °C and 270 ºC, respectively, while utilising an unheated printing bed.

These temperatures were selected based on their significant influence on material viscosity, directly affecting printability and layer adhesion[10]. The choice of layer height plays a crucial role in defining the level of detail and interlayer adhesion in the printed parts, and the software was set to a height of 0.125 mm to optimize the print quality.

A smaller layer height results in finer detailing and stronger interlayer adhesion but increases the printing time. Conversely, a larger layer height reduces printing time but compromises precision and part strength[17]. So, it is essential to optimize these printing according to material characteristics and experimental requirements. This study sets these parameters after multiple tests and adjustments, as initial attempts resulted in inferior composite samples due to fibre discontinuity and poor adhesion between different layers. A total of 12 coupons for each type of test with different combinations of raster angle and infill pattern were fabricated.

The Eiger software from Mark Forged allows multiple types of fiberfill, including concentric, isotropic, all-wall and all-hole. Although the software allows the printing of various infill patterns, the orientation of matrix materials is predefined at + or – 45 degrees. While the fibre can be laid at any different angles as inputted, the matrix material always starts at +45 degrees and is followed by -45 degrees. Figure 2 depicts the 2D view of the orientation of the reinforcement material.

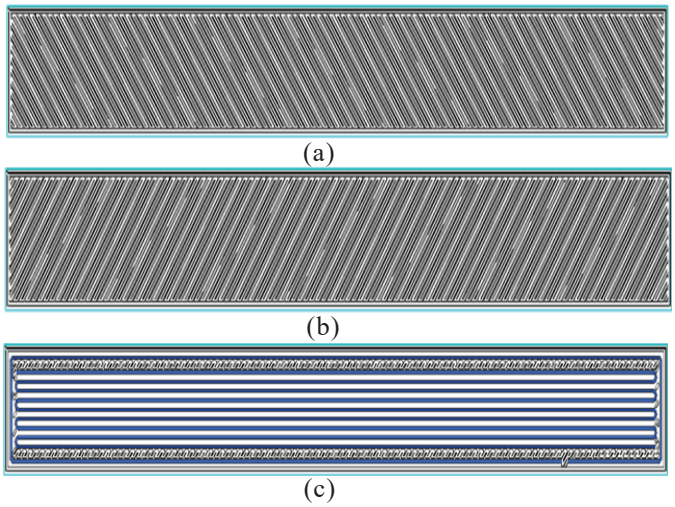


**Figure 2: 2D view of matrix fibre orientation (a) Matrix with Onyx +45°; (b) Matrix with Onyx -45°; and (c) Reinforcement of carbon fibre with isotropic patterns and 1 concentric ring.**

The geometry of the flexural test coupon is based on ASTM D790[23] (see Fig. 3 and Fig. 4 for actual fabricated coupons). According to classical beam theory, the fibres above the neural axis experience compressive stress while those below experience tensile stress. The key principle is that the stress at the neutral axis is zero. For flexural test specimens, the arrangement of carbon fibre layers was guided by this theory, ensuring that no reinforcing fibre was placed at the theoretical centre. Therefore, ten layers of onyx with 0.125 mm each were arranged in the middle. Specifically, four layers of carbon fibre were placed above the central Onyx core, followed by another four layers of carbon fibre below the core. The bottommost and topmost four layers were filled with onyx to keep the fibre from contacting the testing nose. This also makes it easier for the fibres to be deposited and prevents the material from breaking down on the printing bed when the sample is removed. In addition, as recommended by Markforged, two layers of wall with 0.80 mm for the wall sides were provided.

The Impact test coupon's dimensions (see Fig. 5 and Fig. 6 for actual fabricated coupons) were based on ASTM D6110[24], and the fibre arrangement differed from the previous specimen's. Out of the total of one hundred and two layers, the floor and roof were filled with four layers of onyx, similar to that of the previous flexural test specimen. Thirty-four layers of onyx were filled in the middle, and thirty layers of fibres were printed above and below the middle layers. This type of continuous stacking of fibres was chosen ahead of the alternating stacking sequence, which might have one layer of onyx and one layer of Carbon fibre, as these specimens displayed superior energy absorption[25]. This is because, during the printing process, the adhesion between adjacent fibre layers is better than the adhesion between a fibre layer and an onyx layer. Generally, charpy test specimens can be printed in four different ways, notch up, notch down, notch on any of the sides, and vertically built notch. In this work, the up-build orientation was selected as it has proved to have the best performance among all the build orientations[25]. The samples

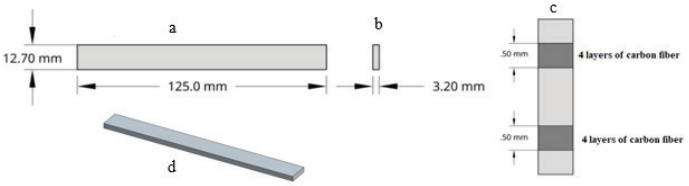


**Figure 3. Geometry view of the coupons for flexural tests (a) front view; (b) side view; (c) top view; and (d) isometric view.**

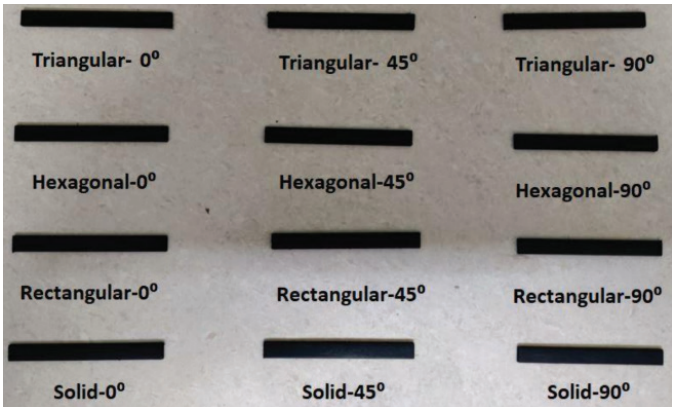


**Figure 4. Fabricated coupons for flexural tests.**

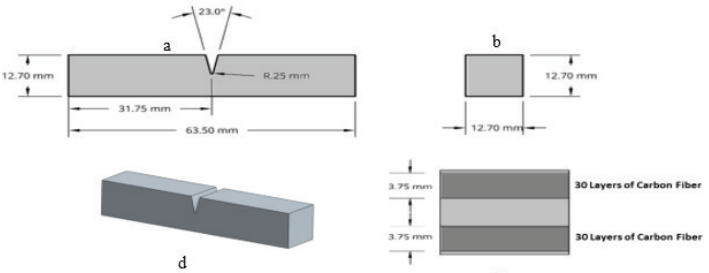


**Figure 5. Geometry view of the coupons for impact tests (a) front view; (b) side view; (c) top view; and (d) isometric view.**

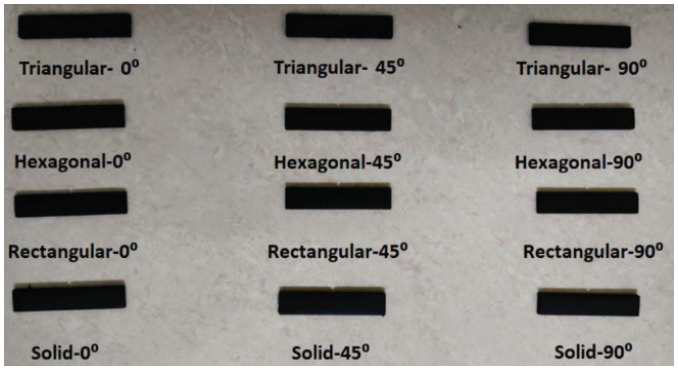


**Figure 6. Fabricated coupons for impact tests.**

were printed identically as per the literature[19], where the length of the coupon was reduced to save printing time and cost.

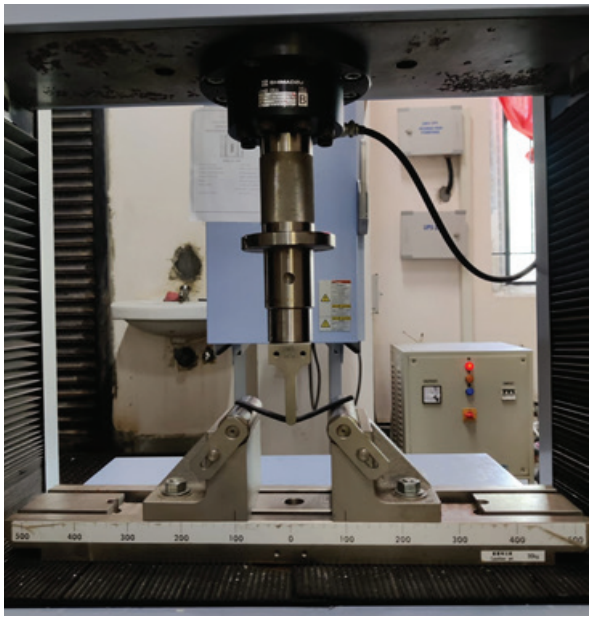

**Figure 7. Impact test machine depicts the images of impact and UTM, respectively, where the coupons were tested for their mechanical properties, developed using the 3D printer.**

## 3. FLEXURAL AND IMPACT TEST

A three-point bending test as per ASTM D790 was carried out with a Universal Testing Machine UTS Shimadzu AG-Xplus 50 KN machine with a 1mm/min displacement rate. The load (F) was applied and the deflection (y) of the specimen was calculated. The flexural strength ($\sigma_f$) and flexural modulus ($E_{flex}$) of the specimen with length (L), breadth (B) and depth (D) was calculated using the following equations respectively.

$$\sigma_f = \frac{3FL}{2BD^2} \tag{1}$$

$$E_{flex} = \frac{FL^3}{4BD^2 y} \tag{2}$$

The Charpy impact test was performed as per ASTM D6110 standards using an Impact Testing Machine. Notched specimens were subjected to a swinging hammer with known mass. The energy absorbed by the material ($I_E$)is noted, and the impact strength of the specimen is calculated using the following Eqn.:

$$\sigma_i = \frac{I_E}{A} \tag{3}$$

## 4. RESULTS AND DISCUSSION

### 4.1 Flexural Test Results - Influence of Raster Angle

Table 1 depicts the results conducted for the flexural test with various raster angles. The outcome of the investigation revealed distinct effects on flexural performance across the composite specimen. With the increase in the raster angle, a reduction in the flexural strength was observed. For example, specimens with a hexagonal infill pattern displayed a flexural strength of 105.448 MPa at a 0° raster angle, which decreased to 59.238 MPa at a 45° angle and further to 51.738 MPa at a 90° angle (Fig. 8). This trend was evident among all the infill pattern types. Generally, 3D printed materials exhibit characteristics similar to laminated structures due to their layer-by-layer construction. The maximum force that a 3D-printed composite can withstand is heavily dependent on the fibre orientation and the direction of force applied. This dependency arises due to the anisotropic nature of these materials.

Therefore, the specimen with a 0° raster angle exhibited higher flexural strength because the deposited fibre layers parallel the bending plane and offer more resistance to the bending force. Similarly, a raster angle of 90º exhibited minimum strength as the loading axis became parallel, and hence, the unbroken fibres at each layer were not able to hold the material together, resulting in failure. The decrease in flexural strength as the raster angle increases could be attributed to the alignment of the print layers and how the internal structure responds to bending forces. At lower raster angles (e.g., 0°), the layers are more aligned with the direction of the applied force, providing better resistance to bending. However, as the raster angle increases, the layer alignment becomes less efficient in resisting bending, leading to reduced flexural strength. This phenomenon highlights the sensitivity of mechanical behaviour to fibre orientation, with higher raster angles introducing inefficiencies in load transfer and stress distribution.

**Table 1. Results of the flexural test**

| Raster angle (°) | Infill pattern | Flexural strength (MPa) | Flexural modulus (GPa) |
|---|---|---|---|
| 0 | Hexagonal | 105.448 | 17.679 |
| 45 | Hexagonal | 59.238 | 4.541 |
| 90 | Hexagonal | 51.738 | 6.698 |
| 0 | Rectangular | 121.058 | 19.403 |
| 45 | Rectangular | 67.207 | 4.799 |
| 90 | Rectangular | 52.386 | 3.196 |
| 0 | Triangular | 116.646 | 21.116 |
| 45 | Triangular | 56.122 | 3.164 |
| 90 | Triangular | 45.346 | 3.533 |
| 0 | Solid | 136.170 | 10.189 |
| 45 | Solid | 57.764 | 6.284 |
| 90 | Solid | 50.283 | 3.378 |

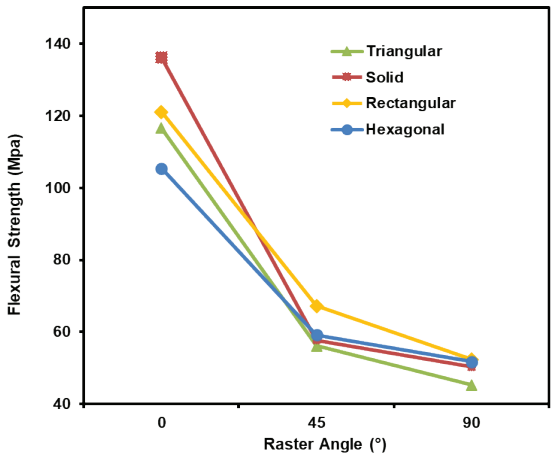


**Figure 8. Comparison plot between flexural strength vs raster angle for various infill patterns.**

### 4.2 Flexural Test Results - Influence of Infill Pattern

The solid infill pattern displayed maximum flexural Strength at 0° raster angle as shown Table 2, displaying an optimal configuration for load distribution along a continuous pathway. The absence of internal voids in solid infill promotes more uniform material distribution and load-bearing capability throughout the specimen. The rectangular-shaped infill consistently demonstrated superior flexural strength ranging from 52.386 MPa at 90° raster angle to 121.058 MPa at 0° raster angle and has lines in both diagonal directions. These lines increase the adhesion and reduce the formation of pores. When the specimen has fewer pores, it has higher structural stability and strength. The 0° raster angle had the highest flexural stiffness of all the infill pattern types, followed by the 45° and 90° raster angles, which showed the lowest flexural stiffness.

### 4.3 Flexural Test Results-Stress Strain Curve

The stress-strain curve is a graphical description of a material's behaviour during the continuous increase of loads. The plot can be generated to investigate its mechanical properties at various loads such as tensile, compression, bending, torsion and shear. The stress-strain curves were directly obtained from the UTM for incremental loads of various specimens of the 3D-printed composite. Figure 9 shows the stress-strain curve for various combinations of infill patterns and raster angles. Specimens with solid infill patterns consistently demonstrated the highest ultimate tensile strength (UTS), with values ranging from 136.170 MPa at 0° raster angle to 50.283 MPa at 90° raster angle. It is evident that the 0° raster angle, irrespective of the infill pattern type, exhibits the highest flexural modulus, indicating stiff behaviour. The stress-strain curve featuring the rectangular infill pattern at a 0° raster angle exhibited an atypical failure mode characterised by a sudden drop in stress immediately after reaching the yield point. Unlike other specimens at the same raster angle, which displayed a gradual plastic deformation post-yield, the rectangular pattern failed abruptly.

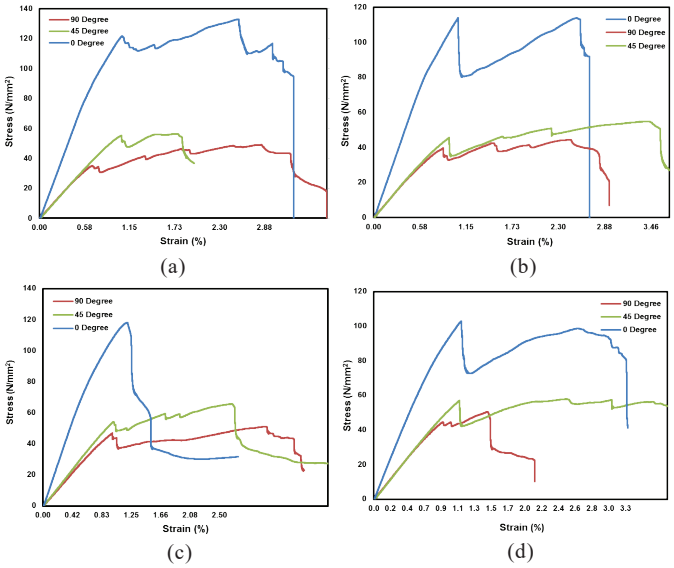


**Figure 9. Stress-strain curves for different infill patterns with three raster angles: (a) solid; (b) hexagonal; (c) rectangle; and (d) triangle.**

### 4.4 Impact Test Results: Influence of Raster Angle

The $45^0$ raster angle displays maximum impact strength followed by $0^0$ as shown Table 2. The specimen with $90^0$ raster angle exhibited the lowest value of impact strength. In general, when the fibre orientation is parallel to the direction of the force, the material exhibits superior structural properties. In this case, though the $0^0$ raster angle was parallel to the direction of force applied, it was laid along the length of the material, which was larger than its width. The $45^0$ raster angle showed better impact resistance than the zero-degree raster angle as the fibres were oriented at an angle to the direction of force applied, and also, the fibres were laid along the width, which was the shorter side.

The $45^0$ infill pattern offers enhanced impact strength due to its diagonal orientation, which helps distribute forces more evenly across the printed part, providing better resistance to both vertical and horizontal impacts compared to patterns aligned with the axes. This orientation also allows for improved load distribution, as the diagonal lines act like beams, absorbing and dispersing forces more effectively than rigid patterns like grid or rectilinear. Additionally, the $45^0$ pattern promotes better layer bonding by creating more overlap points between

adjacent layers, strengthening the material's resistance to shear forces during impacts. In a few cases, specimens with 0º and 45º raster angles had no significant difference in impact strength. The $90^0$ raster angle displayed the lowest value because of the fact that the fibres were laid perpendicular to the direction of force applied.

**Table 2. Impact strength and energy for various infill patterns and raster angle**

| Raster angle (°) | Infill pattern | Impact energy (J) | Impact strength (kJ/m2) |
|---|---|---|---|
| 0 | Hexagonal | 10 | 12.649 |
| 45 | Hexagonal | 10 | 12.649 |
| 90 | Hexagonal | 8 | 10.119 |
| 0 | Rectangular | 12 | 15.178 |
| 45 | Rectangular | 12 | 15.178 |
| 90 | Rectangular | 8 | 10.119 |
| 0 | Triangular | 28 | 35.417 |
| 45 | Triangular | 32 | 40.476 |
| 90 | Triangular | 26 | 32.887 |
| 0 | Solid | 16 | 20.238 |
| 45 | Solid | 20 | 25.298 |
| 90 | Solid | 14 | 12.649 |

### 4.4 Impact Test Results: Influence of Infill Pattern

Figure 10 illustrates the impact forces values of various infill patterns raster angle. From the results, it is evident that the triangular infill pattern displayed maximum impact resistance. This is due to the mesostructure, which balances factor intensity and crack propagation. Unlike the solid infill, the triangular pattern features gaps between the printed lines. These gaps act as disruptions during crack formation. As a crack begins to grow, it encounters these interruptions, forcing it to change direction and resisting its continuous propagation. In the case of the triangular pattern, the interruption of crack propagation in the fracture region helps increase the material's energy-absorbing ability. This can also be due to the solid infill pattern taking much more time to print; hence, the inter-laminar bonding between each layer will be low. Higher printing time will also result in the generation of air gaps and voids, which will further reduce the strength of the material. The hexagon and rectangular infill pattern types depict a lower impact resistance than others; no significant difference was observed in their performance.

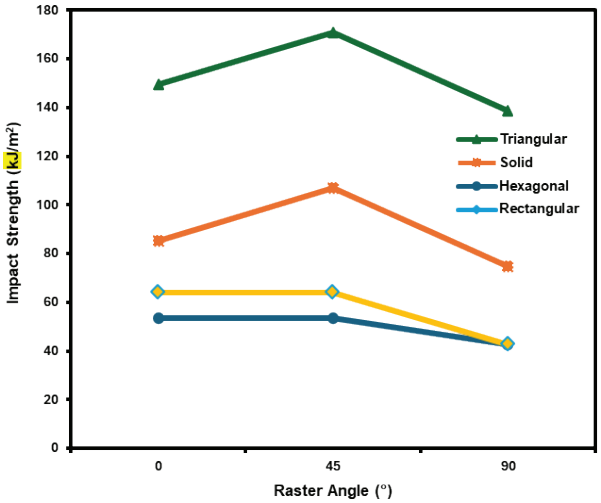


**Figure 10. Variation of Impact strength analysis for different infill patterns and raster angles.**

## 5. COMPARISON WITH EXISTING LITERATURE

The results from the current study on the effects of raster angle and infill pattern on flexural and impact strength align with trends found in existing research, although some differences in specific results are noted. According to the results, flexural strength decreases with increasing raster angle, with the highest strength observed at 0° raster angle. This pattern is consistent with previous studies, such as those by[26-27],who reported similar reductions in strength as raster angles increased. This behavior can be attributed to the anisotropic nature of 3D-printed materials, where the alignment of fibers with the applied load plays a critical role in the material's ability to resist bending forces. In present study, the rectangular infill pattern exhibited the greatest flexural strength at 0°, which supports findings from literature[28] who observed that patterns with diagonal lines enhance material strength due to better adhesion and fewer voids between layers.

Regarding impact strength, the present study results show that the 45° raster angle provided the highest impact resistance, followed by 0° and 90°. This finding matches the results of literature[28-29], where diagonal orientations, such as 45°, improve impact resistance by distributing forces more effectively. Conversely, 90° raster angles resulted in the lowest impact strength, which has been similarly reported in literature[30] who explained that this orientation weakens the material's ability to resist impact forces due to the perpendicular alignment of the fibers to the applied force. Furthermore, the present study found that the triangular infill pattern outperformed others in terms of impact resistance, which is consistent with research by literature[31], who highlighted that patterns like triangles, which introduce interruptions in crack propagation, are more effective at energy dissipation.

Although solid infill patterns provided high flexural strength, their impact resistance was relatively lower compared to the triangular pattern, corroborating findings from literature[30] who noted that solid patterns tend to have lower energy-absorbing capacity due to weaker inter-layer bonding and the potential formation of voids. Overall, the current results align well with the existing literature, confirming that raster angle and infill pattern significantly influence the mechanical performance of 3D-printed materials, with fiber orientation and pattern geometry playing crucial roles in determining the material's response to various loading conditions

## 5. CONCLUSION

Given the rapid rate at which additive manufacturing is evolving, it is critical to fully understand the variables that affect the mechanical characteristics of 3D-printed composites. This research addresses this need and provides a better understanding of how changes in infill pattern and raster angle affect the flexural and impact behaviour of onyx carbon fibre-reinforced composites. The composite comprises onyx as the matrix material and carbon fibre as the reinforcement

material. The samples were additively manufactured using fused filament fabrication technology in 12 different combinations of infill patterns and raster angles. Due to the anisotropic nature of 3D printed composites, significant variations in mechanical properties were expected. Confirming the hypothesis, the fibre layup orientation and infill pattern significantly impacted the flexural and impact strength of a material. From the findings, it is possible to conclude that a 0° raster angle with either solid or rectangular infill patterns is optimal for applications requiring high flexural strength. At the same time, $45^0$ raster angles with either triangular or solid patterns are ideal for applications where high impact resistance is required. Future researchers may explore various specimen varieties, angles, and printing technologies for a more comprehensive analysis.

## REFERENCES


1. ASTM International. ASTM F2792–12a: Standard terminology for additive manufacturing technologies. West Conshohocken (PA): ASTM International; 2015.
2. Krenkel W. Carbon fibre reinforced silicon carbide composites (C/SiC, C/C-SiC). In: Bansal NP, editor. Handbook of ceramic composites. Boston (MA): Springer; 2006. p. 117–148.
3. Koniuszewska AG, Kaczmar JW. Application of polymer based composite materials in transportation. Prog Rubber Plast Recycling Technol. 2016;32:1–23.
4. Adam H. Carbon fibre in automotive applications. Material Design. 1997;18(4–6):349–55 .ISSN: 02613069
5. Kumar A, Lal Krishna G, Anantha Subramanian V. Design and Analysis of a Carbon Composite Propeller for Podded Propulsion. In: Murali K, Sriram V, Samad A, Saha N, editors. Proceedings of the Fourth International Conference in Ocean Engineering (ICOE2018). Singapore: Springer; 2019. (Lecture Notes in Civil Engineering; vol. 22).
6. Chacón JM, Caminero MA, Núñez PJ, García-Plaza E, García-Moreno I, Reverte JM. Additive manufacturing of continuous fibre reinforced thermoplastic composites using fused deposition modelling: Effect of process parameters on mechanical properties. Compos Sci Technol. 2019;181:107688.
7. Van Der Klift F, Koga Y, Todoroki A, Ueda M, Hirano Y. 3D printing of continuous carbon fibre reinforced thermoplastic (CFRTP) tensile test specimens. Open Journal of Composite Material. 2016;6(1):18–27.
8. Melenka GW, Cheung BKO, Schofield JS, Dawson MR, Carey JP. Evaluation and prediction of the tensile properties of continuous fibre-reinforced 3D printed structures. Composite Structures. 2016;153:866–75. doi:10.1016/j.compstruct.2016.07.018
9. Qayyum H, Hussain G, Sulaiman M, Hassan M, Ali A, Muhammad R, et al. Effect of raster angle and infill pattern on the in-plane and edgewise flexural properties of fused filament fabricated acrylonitrile–butadiene–styrene. Applied Sciences. 2022;12(24):12690.
10. Hu Q, Duan Y, Zhang H, Liu D, Yan B, Peng F, et al. Manufacturing and 3D printing of continuous carbon fibre prepreg filament. Journal of Materials Science. 2018;53(3):1887–98.
11. Pyl L, Kalteremidou KA, Van Hemelrijck D. Exploration of specimen geometry and tab configuration for tensile testing exploiting the potential of 3D printing freeform shape continuous carbon fibre-reinforced nylon matrix composites. Polymer Test. 2018;71:318–28.
12. Zakaria H, Khan SF, Fee MFC, Ibrahim M. Printing temperature, printing speed and raster angle variation effect in fused filament fabrication. IOP Conf Ser Mater Sci Eng. 2019;670.
13. Martín MJ, Auñón JA, Martín F. Influence of infill pattern on mechanical behavior of polymeric and composites specimens manufactured using fused filament fabrication technology. Polymers. 2021;13:2934.
14. Srinivasan R, Kumar KN, Ibrahim AJ, Anandu K, Gurudhevan R. Impact of fused deposition process parameter (infill pattern) on the strength of PETG part. Mater Today Proc. 2020;27:1801–5.
15. Ning F, Cong W, Wei J, Wang S, Zhang M. Additive manufacturing of CFRP composites using fused deposition modelling: Effects of carbon fibre content and length. In: Int Manuf Sci Eng Conf. 2015 Jun 8;56826:V001T02A067.
16. Ghebretinsae F, Mikkelsen O, Akessa A. Strength analysis of 3D printed carbon fibre reinforced thermoplastic using experimental and numerical methods. IOP Conf Ser Mater Sci Eng. 2019;012024.
17. Hu Q, Duan Y, Zhang H, Liu D, Yan B, Peng F. Manufacturing and 3D printing of continuous carbon fibre prepreg filament. J Mater Sci. 2017;53(3):1887–98.
18. Prajapati AR, Dave HK, Raval HK. Effect of fibre volume fraction on the impact strength of fibre reinforced polymer composites made by FDM process. Mater Today Proc. 2021;44(1):2102–6.
19. Hetrick DR, Sanei SH, Ashour O, Bakis CE. Charpy impact energy absorption of 3D printed continuous Kevlar reinforced composites. J Compos Mater. 2021;55(12):1705–13.
20. Pop MA, Zaharia SM, Chicos LA, Lancea C, Stamate VM, Buican GR. Effect of the infill patterns on the mechanical properties of the carbon fibre 3D printed parts. IOP Conf Ser Mater Sci Eng. 2022;1235(1):01.
21. Daly M, Tarfaoui M, Bouali M, Bendarma A. Effects of infill density and pattern on the tensile mechanical behavior of 3D-printed glycolyzed polyethylene terephthalate reinforced with carbon-fiber composites by the FDM process. J Compos Sci. 2024;8(4):115.
22. Nguyen-Van V, Peng C, Tran P, Wickramasinghe S, Do T, Ruan D. Mechanical and dynamic performance of 3D-printed continuous carbon fibre Onyx composites. Thin-Walled Struct. 2024;201:111979.
23. ASTM International. ASTM D790-02: Standard test methods for flexural properties of unreinforced and reinforced plastics and electrical insulating materials. West Conshohocken (PA): ASTM International; 2002.
24. ASTM International. ASTM D6110-18: Standard test method for determining the Charpy impact resistance of notched specimens of plastics. West Conshohocken (PA):

ASTM International; 2018.
25. Caminero MA, Chacón JM, García-Moreno I, Rodríguez GP. Impact damage resistance of 3D printed continuous fibre reinforced thermoplastic composites using fused deposition modelling. Compos B Eng. 2018;148:93–103.
26. Gibson I, Rosen D, Stucker B, Khorasani M. Additive manufacturing technologies. Cham (Switzerland): Springer; 2021. Vol. 17. p. 160–86.
27. Yasmin M, Iqbal J, Khan Z. Influence of raster angle on the flexural strength and fracture toughness of FDM printed parts. J Mater Sci. 2019;54(1):201–10.
28. Muthuraj R, Sivasubramanian S, Rajendran S. Investigation on mechanical properties of 3D printed PLA parts with different infill patterns and orientations. Mater Today Proc. 2020;28(1):87–92.
29. Koch J, Wright PK, Moore S. The effect of build orientation on mechanical properties of 3D printed parts. J Manuf Process. 2017;28:108–16.
30. Sharma P, Singh R. Effect of infill density and orientation on mechanical properties of 3D printed parts. Int J Adv Manuf Technol. 2018;95(1–4):221–30.
31. Singh R, Verma R, Sharma P. Effect of infill pattern on mechanical and thermal properties of FDM printed parts. J Thermoplast Compos Mater. 2019;32(3):271–83.

## CONTRIBUTORS

**Dr Ashok Kumar** obtained his PhD in Naval Architecture and Ocean Engineering at the Department of Ocean Engineering, Indian Institute of Technology Madras (IITM). His research interests include: Ship design, hydrodynamics, propellers, composite materials, motion analysis of floating structures.
In the current study he contributed to the original draft preparation, edition and reviewed the manuscript

**Mr Ashwin Kumar** obtained his Bachelor's in Mechanical Engineering at the Department of Mechanical Engineering, Easwari Engineering College, Ramapuram, Chennai. His areas of interest include: Additive manufacturing, composite materials, engineering optimisation, and robotics.
In the current study he investigated the research topic, developed the methodology, performed formal analysis and visualisation, wrote the original draft, edited, and reviewed the manuscript.